

Replication Protein A Interactions with DNA. 1. Functions of the DNA-Binding and Zinc-Finger Domains of the 70-kDa Subunit[†]

André P. Walther, Xavier V. Gomes,[‡] Ye Lao, Chang Geun Lee, and Marc S. Wold*

Department of Biochemistry, University of Iowa College of Medicine, 51 Newton Road, Iowa City, Iowa 52242-1109

Received October 2, 1998; Revised Manuscript Received January 8, 1999

ABSTRACT: Human replication protein A (RPA) is a multiple subunit single-stranded DNA-binding protein that is required for multiple processes in cellular DNA metabolism. This complex, composed of subunits of 70, 32, and 14 kDa, binds to single-stranded DNA (ssDNA) with high affinity and participates in multiple protein–protein interactions. The 70-kDa subunit of RPA is known to be composed of multiple domains: an N-terminal domain that participates in protein interactions, a central DNA-binding domain (composed of two copies of a ssDNA-binding motif), a putative (C-X₂-C-X₁₃-C-X₂-C) zinc finger, and a C-terminal intersubunit interaction domain. A series of mutant forms of RPA were used to elucidate the roles of these domains in RPA function. The central DNA-binding domain was necessary and sufficient for interactions with ssDNA; however, adjacent sequences, including the zinc-finger domain and part of the N-terminal domain, were needed for optimal ssDNA-binding activity. The role of aromatic residues in RPA–DNA interactions was examined. Mutation of any one of the four aromatic residues shown to interact with ssDNA had minimal effects on RPA activity, indicating that individually these residues are not critical for RPA activity. Mutation of the zinc-finger domain altered the structure of the RPA complex, reduced ssDNA-binding activity, and eliminated activity in DNA replication.

Replication protein A is a heterotrimeric single-stranded DNA-binding protein that is required for multiple processes in DNA metabolism including DNA replication, DNA repair, and recombination (reviewed in 1). Human RPA (RPA)¹ is a stable complex of three subunits with molecular masses of 70, 32, and 14 kDa (RPA70, RPA32, and RPA14, respectively) (2, 3). RPA is highly conserved throughout evolution, and homologous, heterotrimeric single-stranded DNA-binding proteins have been identified in all eukaryotes examined (1, 4). Despite a high degree of homology, only some RPA homologues can substitute for human RPA in SV40 DNA replication, suggesting that there are species-specific interactions required for RPA function (5–8).

RPA interacts with proteins required for the initiation of DNA replication (SV40 T antigen, DNA polymerase α) (1, 9), the damage recognition and excision steps of nucleotide excision repair (XPA and XPG) (10–12), homologous recombination (Rad51 and Rad52) (13–16), regulation of transcription (GAL4 and VP16), and regulation of the cell cycle (p53) (17–21). These protein interactions are important for RPA function in the cell. Recent studies indicate that

RPA–protein interactions modify protein activity and can change in response to cellular signals (20–22; Braun et al., in preparation). RPA also becomes phosphorylated during cellular DNA metabolism (reviewed in 1). Recent studies have suggested that this phosphorylation modulates RPA activity by affecting RPA–protein interactions (Braun et al., in preparation).

RPA binds to single-stranded DNA (ssDNA) with high affinity ($K_a \sim 10^{10} \text{ M}^{-1}$) and low cooperativity (24–26); binding is nonspecific with a preference for binding pyrimidine-rich sequences (24, 27). RPA forms a stable complex with DNA that has an occluded binding site size of 30 nucleotides (24–26). A second unstable complex with an apparent occluded binding site size of 8–10 nt has been observed in studies using chemical cross-linking (28, 29). Most RPA homologues have similar binding properties (1); although, the DNA-binding properties of the homologue from *S. cerevisiae* differ significantly from human RPA (27). Recently, it has been shown that a complex of 32- and 14-kDa subunits of RPA can interact weakly with ssDNA (27, 30–32). The affinity of this complex for ssDNA is at least 5 orders of magnitude lower than that of the heterotrimeric RPA complex (27). It is not yet known how this weak binding activity contributes to the overall activity of RPA.

Deletion and mutational analyses have identified four domains in RPA70: an N-terminal domain (residues 1–168) that participates in RPA–protein interactions, a central DNA-binding domain (residues 169–441), a putative C₄-type zinc-finger motif (residues ~481–503), and a C-terminal domain (~503–616) which is required for interactions with the 32- and 14-kDa subunits of RPA [reviewed in (1, 22)]. The structure of the central DNA-binding domain has been

[†] These studies were supported by Grant GM44721 from the National Institutes of Health General Medicine Institute.

* To whom correspondence should be addressed. Telephone: (319) 335-6784. Fax: (319) 335-9570. Email: marc-wold@uiowa.edu.

[‡] Current address: Department of Biochemistry and Molecular Biophysics, Washington University, School of Medicine, St. Louis, MO 63110-1093.

¹ Abbreviations: RPA, human replication protein A; RPA70, 70-kDa subunit of RPA; RPA32, 32-kDa subunit of RPA; RPA14, 14-kDa subunit of RPA; ssDNA, single-stranded DNA; XPA, *Xeroderma pigmentosum* group A protein; DTT, dithiothreitol; GMSA, gel mobility shift assay; SDS–PAGE, SDS–polyacrylamide gel electrophoresis; ELISA, enzyme-linked immunosorbent assay; nt, nucleotide; bp, base pair; SSB, single-stranded DNA-binding protein.

determined and is composed of two copies of an oligonucleotide/oligosaccharide-binding (OB) fold (33). The structures of these two motifs are similar to each other and to those found in other single-stranded DNA-binding proteins with an OB-fold (33). A third sequence with homology to the DNA-binding motifs has been identified in the central region of the 32-kDa subunit of RPA (34). Although its structure has not been determined, this domain is probably responsible for the weak DNA-binding activity observed with RPA 32 (27, 30–32, 34). In the crystal structure, multiple interactions were observed between the high-affinity DNA-binding domain and the DNA (33). These interactions included hydrogen bonds with individual bases and the phosphate backbone as well as hydrophobic interactions between several aromatic residues and individual bases. It is currently not known what the individual contributions of these interactions are to the overall binding affinity of RPA.

The putative C₄-type zinc-finger motif (residues 481–503) is conserved in all RPA70 homologues (1, 4). While it has been suggested that the zinc-finger motif may be involved in binding to damaged DNA (35), its function is currently not known. There has been no quantitative analysis of the role of this domain in RPA–DNA interactions. In addition, previous functional analyses of this motif have been ambiguous with different laboratories obtaining contradictory results regarding the role of this motif in replication and DNA repair (36–39) (see Discussion).

We have examined the roles of the central DNA-binding domain, the putative zinc-finger domain, and other regions of RPA70. Using multiple mutant forms of RPA, we show that the central DNA-binding domain is necessary but not sufficient for optimal ssDNA binding. Sequences adjacent to this domain are necessary for high-affinity DNA-binding activity. Mutation of aromatic residues F269 and F386 in the central DNA-binding domain had modest effects on RPA DNA-binding activity and on RPA's ability to support DNA replication. In contrast, mutation of aromatic residues F238 and W361 caused a ≥ 500 -fold reduction in ssDNA-binding activity and a perturbation of the structure of RPA. This structural perturbation also disrupted interactions with SV40 T antigen but did not affect interaction with XPA protein. We also examined the role of the zinc-finger motif and show that mutation of this motif reduced RPA ssDNA-binding activity by an order of magnitude and caused loss of activity in DNA replication. We also show that this mutation disrupts the structure of the C-terminus of RPA, suggesting that this domain plays a role in these processes.

MATERIALS AND METHODS

Materials. Restriction endonucleases, polynucleotide kinase, and Klenow fragment were purchased from New England BioLabs and Life Technologies, Inc. PFU DNA polymerase was purchased from Stratagene. [γ -³²P]ATP (4500 Ci/mmol) and [α -³²P]dATP (3000 Ci/mmol) were obtained from Amersham. Oligonucleotides were synthesized by the DNA core facility at the University of Iowa. *E. coli* DH5 α cells were from Life Technologies, Inc. *E. coli* expression strain BL21(DE3) was from W. Studier (40). Oligodeoxythymidine [(dT)₃₀] was purchased from Biosynthesis, Inc.

HI buffer contains 30 mM HEPES (diluted from 1 M stock at pH 7.8), 1 mM dithiothreitol, 0.25 mM EDTA, 0.5% (w/

v) inositol, and 0.01% (v/v) Nonidet-P40. HI was supplemented with different concentrations of salt as indicated. 1 \times Tris acetate/EDTA (TAE) gel buffer contained 40 mM Tris–acetate and 2 mM EDTA, pH 8.5 (41).

RPA expression plasmids (p11d-tRPA, p11d-RPA70, and pSD-RPA14/32) were described previously (42).

DNA Manipulation. Restriction endonucleases and Klenow were used according to the manufacturers' recommendations. Oligonucleotides were radiolabeled with [γ -³²P]ATP using polynucleotide kinase (41). Polymerase chain reactions (PCR) were performed with Vent DNA polymerase (New England Biolabs) in a DNA Thermal Cycler (Perkin-Elmer). DNA amplification conditions were 29 cycles of 94 °C for 1 min; 55 °C for 1 min; 72 °C for 3 min. PCR products and DNA fragments were isolated from 1% TAE agarose gels using a GeneClean II kit (BIO 101, La Jolla, CA) according to manufacturer's specifications. Ligation reactions and transformations were according to Ausubel and co-workers (41). Recombinant plasmids were transformed into strain *E. coli* DH5 α and isolated by the boiling lysis method (41). All mutations were confirmed by DNA sequencing at the DNA core facility at the University of Iowa.

Proteins Used in These Studies. Multiple mutant forms of RPA are used in these studies (all are shown schematically in Figure 1). Either these forms have been described previously (22, 42–44) or their construction is described below. Protein nomenclature: Complexes of multiple subunits are indicated by RPA• followed by a description of the sequences modified. Deletions are indicated by Δ XX–XX with the numbers referring to the residues deleted. When only a portion of a protein is present, the mutant form is named for the amino acids present; for example, RPA70-(113–441) contains residues 113 through 441 of RPA70 (residues 1 through 112 and residues 442 through 616 of wild-type RPA70 are deleted). Point mutations are indicated using one-letter amino acid abbreviations and the residue number. Abbreviations used are described in Figure 1.

Construction of RPA70 DNA-Binding Domain Mutants. A series of mutants were constructed with different regions of the N- and C-termini of RPA70 deleted. PCR was used to amplify specific regions of the RPA70 cDNA (Figure 1). The N-terminal primers were designed to introduce nucleotide base changes (underlined) to generate a *Bam*HI restriction site followed by a *Nco*I restriction site: 5'-GGAG-GATCCATGGGCAATCCAGTG-3' (RPA70 Δ 1–112); 5'-TTTGGATCCATGGCAGGTCCCAGC-3' (RPA70 Δ 1–168). The *Nco*I restriction site provided the ATG initiation codon. The primers used to generate deletion at the C-termini were designed such that primers contained nucleotide base changes (underlined) that generated a *Bam*HI restriction site and a termination codon: 5'-CAAGGATCCTCAGTTGGTGTT-3' (RPA70 Δ 442–616); 5'-CGGGCAGGATCCTTACATG-CAGTT-3' (RPA70 Δ 477–616); 5'-TTGGGATCCTTAG-GTGTGCA-3' (RPA70 Δ 507–616). Appropriate N- and C-terminal primers were used to amplify different regions of the central region of the RPA70 cDNA. Amplified sequences were digested with *Bam*HI and *Nco*I, isolated, and ligated to pET-11d digested with *Bam*HI and *Nco*I. (In some cases, PCR products were initially inserted into pUC19 and then subcloned into pET-11d.) The resulting series of expression vectors contained specific deletions of the RPA70 gene at the N- and C-termini. Each plasmid contained a T7

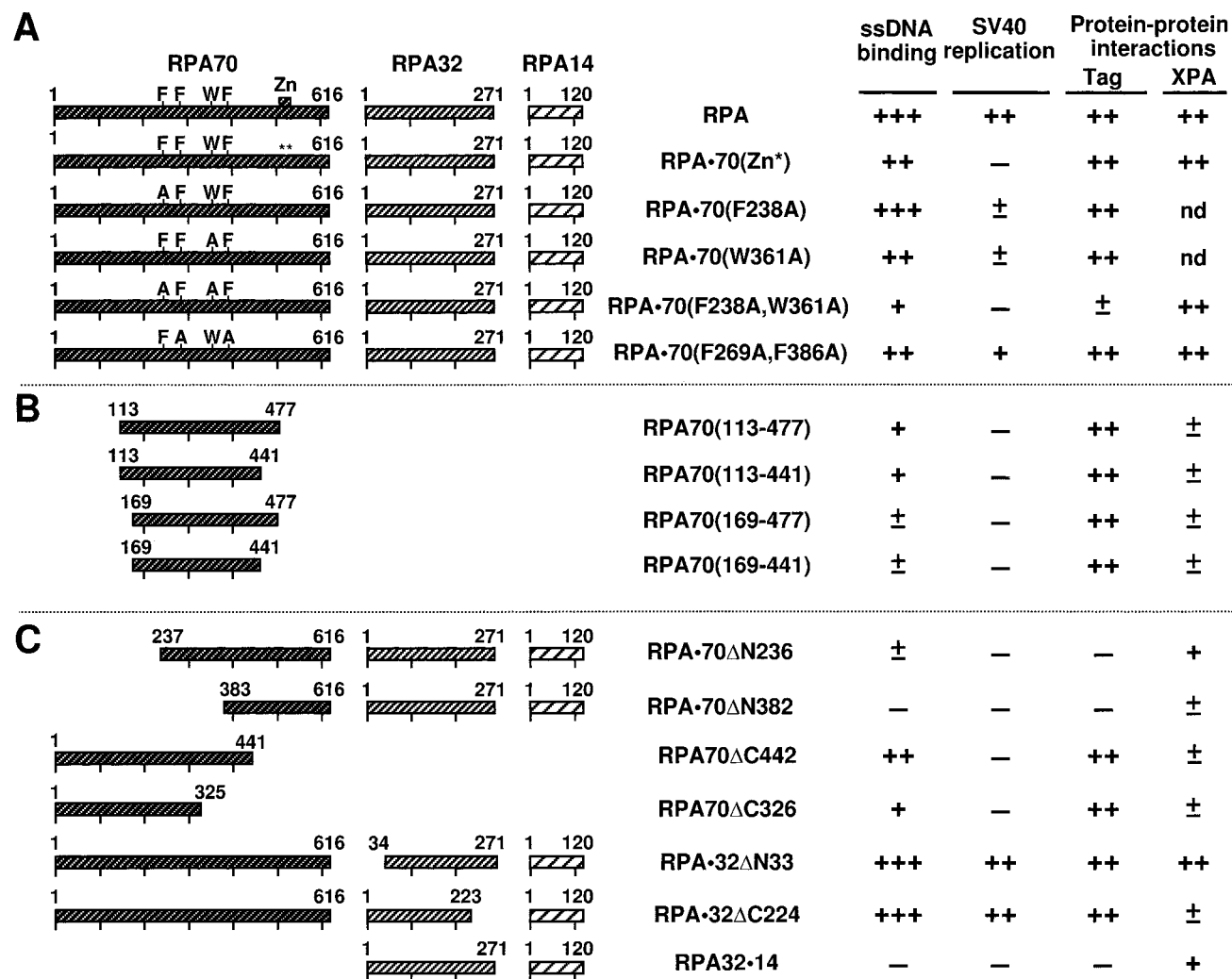


FIGURE 1: Mutant forms of RPA used in these studies. The left portion shows schematic diagrams of all RPA mutants used in this study: (A) wild-type RPA, RPA-70(Zn*), and aromatic residue mutants; (B) DNA-binding domain polypeptides; (C) deletion mutants described previously (22, 44). Beginning and ending amino acids of each mutant are indicated. Aromatic residues and mutations made are indicated by letters. Ticks indicate positions every 100 amino acids, and the position of the putative zinc-finger motif is indicated by a box (Zn). The activities of each of the mutants in relation to wild-type RPA are shown to the right. ssDNA-binding activity was determined in these studies or (27, 44) with (+++) wild-type binding, (++) binding reduced by a order of magnitude, (+) binding reduced by 2 orders of magnitude, (±) binding reduced by 3 orders of magnitude, and (—) binding reduced by more than 4 orders of magnitude. SV40 DNA replication activity was determined in these studies or previously (43, 44). Protein interactions with T antigen or DNA polymerase α were determined by ELISA in these studies. The number of (+) marks indicates the relative activity, (±) indicates minimal activity, (—) indicates no activity, and nd indicates not determined. The following RPA mutants were used in these studies (abbreviations where used are listed in brackets): wild-type RPA [RPA], RPA-70(C500S,C503S) [RPA-70(Zn*)], RPA-70(F238A), RPA-70(W361A), RPA-70(F238A,W361A), RPA-70(F269A,T270S,F386A) [RPA-70(F269A,F386A)], RPA-70Δ1–236 [RPA-70ΔN236], RPA-70Δ1–382 [RPA-70ΔN382], RPA70Δ442–616 [RPA70ΔC442], RPA70Δ326–616 [RPA70ΔC326], RPA70(113–477), RPA70(113–441), RPA70(169–477), RPA70(169–441), RPA-32Δ1–33 [RPA-32ΔN33], RPA-32Δ224–270 [RPA-32ΔC224], and RPA32-14.

promoter, a Shine–Dalgarno ribosome-binding site, and the coding sequence of a RPA70 deletion mutant.

Construction of RPA70(C500S,C503S). A set of two internal PCR primers was constructed to introduce point mutations in the coding sequence of the RPA70 gene. These point mutations alter two of the four cysteines of the putative “zinc-finger” motif. The primer 5′-CTTCTCCGATCGG-TACAATCC-3′ (C500S-Zrev) contained nucleotide changes (underlined) to alter cysteine 500 to a serine while primer 5′-TTGTACCGATCGGAGAGAAGTCCGAC-3′ (C500S-Zfor) contained nucleotide changes (underlined) that changed cysteine 500 to serine and cysteine 503 to serine and generated a *PvuI* restriction site at residue 500. An N-terminal PCR primer (5′-CCAGGATCCGTACGGCGTA-GAGGA-3′) (pET- ϕ 10) and a C-terminal PCR primer (5′-

ATGCTAGTTATTGCTCAGCGG-3′) (#35) were also used. The pET- ϕ 10 sequence is located immediately upstream of the T7 RNA polymerase promoter in the pET11d (40). Primer #35 is downstream of the *Bam*HI site in the pET11d. The primer pairs C500S-Zrev with pET- ϕ 10 and C500S-Zfor with #35 were used to amplify ~1500 and ~900 bp fragments, respectively, of the coding sequence of RPA70 from plasmid p11d-RPA70 (42). These fragments were individually ligated into pUC19 digested with *Sma*I to generate plasmids pUC19-RPA70(1–500:C500S) and pUC19-RPA70(500–616:C500S,C503S), respectively. pUC19-RPA70(1–500:C500S) was digested with *Nco*I and *Pvu*II to produce a ~1490 bp fragment. pUC19-RPA70(500–616:C500S,C503S) was digested with *Pvu*II and *Bam*HI to generate a ~840 bp fragment. Each fragment was isolated

and ligated to pET-11d digested with *Bam*HI and *Nco*I. The subsequent vector, p11d-RPA70(C500S,C503S), contained the coding sequence of RPA70 with nucleotide changes which altered cysteine 500 to serine and cysteine 503 to serine. Sequence analysis confirmed the presence of the two point mutations.

A vector capable of expressing RPA32, RPA14, and mutant RPA70(C500S,C503S) was constructed using a procedure similar to that used to generate p11d-tRPA (42). pSD-RPA14/32 was digested with *Bam*HI, *Aat*II, and *Alw*NI restriction enzymes, generating a 2.25 kb *Bam*HI–*Aat*II fragment containing the coding sequences of both RPA14 and RPA32. This 2.25 kb fragment was ligated to p11d-RPA70(C500S,C503S) that had been digested with *Bam*HI and *Aat*II. The resulting plasmid, ptRPA•70(C500S,C503S), contains a single T7 RNA polymerase promoter followed by the coding sequence of the mutated 70-kDa subunit and the wild-type 14- and 32-kDa subunits of RPA. Each coding sequence is preceded by a Shine–Dalgarno ribosome-binding site.

Construction of RPA70 Aromatic Residue Mutants. Conserved aromatic residues present in RPA70 were mutated using the QuikChange Site-Directed Mutagenesis protocol (Stratagene). Individual aromatic residues were mutated to alanines using the following primer pairs: 5′-ATCCGAGC-TACGCGCCCAATGAGCAAGTG-3′ and 5′-CACTTGCT-CATTGGCGGCCGTAGCTCGGAT-3′ (RPA70 F238A creating an *Eag*I site); 5′-AACAAGCAGGCTAGCGCTGTT-AAAAATGAC-3′ and 5′-TTTAACAGCGCTAGCGCTGCT-TGTTAGCAAT-3′ (RPA70 F269A, T270S creating a *Nhe*I site); 5′-GTGACTGCTACGCTAGCGGGGGAAGATGCT-3′ and 5′-AGCATCTTCCCCCGCTAGCGTAGCAGTCAC-3′ (RPA70 W361A creating a *Nhe*I site); 5′-GTCTCTGAT-GCCGGCGGACGGAGCCTCTCC-3′ and 5′-GCTCCGT-CCGCGGCATCAGAGACTCGGGC-3′ (RPA70 F386A creating a *Nae*I site). Residues F269/T270 and F386 were individually mutated in the vector pET11d-RPA70 to generate pET11d-RPA70 F269A,T270S and pET11d-RPA70 F386A. The 14- and 32-kDa subunits were added on a *Bam*HI–*Pvu*I fragment isolated from pSD-RPA14/32 (44) to generate the triple-expression vectors ptRPA•70 F269A and ptRPA•70 F386A, respectively. Mutations F269A/T270S and F386A were also generated in tandem by ligation of the *Xho*I–*Sac*I fragment from ptRPA•70(F386A) into ptRPA•70(F269A/T270S) digested with *Xho*I and *Sac*I, yielding ptRPA•70(F269A/T270S, F386A). Residues F238 and W361 were individually mutated in the vector p11d-tRPA (42) to generate ptRPA•70(F238A) and ptRPA•70(W361A). Mutations F238A and W361A were generated in tandem by QuikChange Site-Directed Mutagenesis using F238A primers and ptRPA•70(W361A) as the template vector, yielding ptRPA•70(F238A,W361A).

Induction and Purification of Mutant Forms of RPA. The various deletion mutants were expressed in BL21(DE3) cells as described previously (42, 44). Purification of RPA70 mutants followed previously published procedures in which *E. coli* lysates are fractionated over Affi-gel Blue, hydroxylapatite (HAP), and Mono-Q columns (42, 44). During the purification, forms of RPA were monitored by immunoblotting (45). Like wild-type RPA, the deletion mutants RPA70(113–441), RPA70(113–477), RPA70(169–441),

and RPA70(169–477) eluted in 1.5 M NaSCN from Affi-gel Blue and at low (40 mM) potassium phosphate from HAP. When these proteins were applied to a Mono-Q (HR5/5) column (Pharmacia) equilibrated with HI buffer containing 14 mM KCl, none of them bound to the column; however, most of the impurities were retained on the column. The flow-through fractions for each protein were mixed 1:2 with 2 M sodium thiocyanate and loaded separately onto a 5 mL HAP column equilibrated with HI buffer. The column was washed sequentially with 15 mL each of HI buffer containing 0, 40, 80, and 100 mM potassium phosphate. Each DNA-binding domain mutant bound to the column and was eluted in HI buffer with ~40 mM potassium phosphate. All heterotrimeric aromatic mutants were purified in a manner similar to wild-type RPA as described previously (42). The elution profiles of the aromatic mutants were similar to wild-type RPA. The RPA complex containing two cysteines mutated in the putative zinc-finger motif [RPA•70(Zn*)] was purified as described above except that it was eluted from Mono-Q in ~200 mM KCl. Protein concentrations were determined by Bradford assay using bovine serum albumin as a standard (46).

Gel Mobility Shift Assays. Gel mobility shift assays were performed as described previously with slight modifications (24). Binding assays were carried out in 15 μ L binding reactions in HI buffer containing in 1 \times FBB buffer [30 mM HEPES (pH 7.8), 100 mM NaCl, 5 mM MgCl₂, 0.5% inositol, and 1 mM DTT]. Increasing amounts of RPA were incubated with 2 fmol of radiolabeled oligonucleotides and 50 ng/ μ L BSA at 25 °C for 20 min. Binding reactions were brought to a final concentration of 4% glycerol and 0.01% bromophenol blue and electrophoresed on 1% agarose gel in 0.1 \times TAE at 100 V/cm for 1.5 h. The gels were then dried on DE81 paper, and radioactive bands were visualized by autoradiography. The radioactivity in each band was quantitated using a Packard Instant Imager. The data were analyzed by nonlinear least-squares fitting to the Langmuir binding equation using Kaleidagraph (Abelbeck Software) as described previously (25).

Enzyme-Linked Immunosorbent Assay (ELISA). ELISA to examine interactions between purified proteins were carried out as described previously (22, 47). The 96-well microtiter plates were coated with 10 pmol of RPA or a RPA mutant and incubated for 1 h at 25 °C. Plates were washed 3 times with phosphate-buffered saline (PBS) containing 0.2% Tween-20 (all washes are 3 times with PBS+Tween). The plates were then blocked with 5% milk in PBS for 10 min at 25 °C, washed, and incubated with the indicated amount of either SV40 large T antigen, XPA protein, or BSA in PBS with 5% milk for 1 h at 25 °C. The plates were washed, incubated with either anti-T antigen (419) (48) or anti-polyHistidine (HIS-1; Sigma) antibodies in PBS with 5% milk for 30 min at 25 °C, and washed again. Antibody was detected using anti-mouse IgG peroxidase conjugate (Sigma) developed after incubation at 25 °C in 0.8 mg/mL *o*-phenylenediamine in 0.05 M phosphate–citrate buffer with 0.03% sodium perborate. OD₄₅₀ was quantitated multiple times between 20 and 60 min using a microtiter plate reader to confirm the linearity of the assay and the consistency of individual readings.

RESULTS

Initial Characterization of Mutant Forms of RPA. Previous mutational and structural analyses of RPA70 have shown that there is a central DNA-binding domain between residues 169 and 441 (1). This domain contains two copies of a ssDNA-binding motif that interacts directly with ssDNA (33). The N-terminal binding motif also participates in RPA–protein interactions (22). Two series of mutant forms of RPA were generated to examine the specific role of the central binding domain in RPA function. In the first series, various combinations of conserved aromatic residues in the two ssDNA-binding motifs were mutated to alanine (Figure 1A). In the second series, the central DNA-binding domain was expressed with various combinations of adjacent sequences (Figure 1B). These two series will be referred to as the aromatic residue mutants and DNA-binding domain polypeptides, respectively. In addition, a mutant form of RPA was made in which two of the conserved (C500 and C503) cysteine residues in the putative zinc-finger motif in RPA70 were mutated to serine [RPA•70(Zn*); Figure 1A].

Each of the mutant forms of RPA70 was expressed in *E. coli*, and their properties were examined. Full-length forms of RPA70 were insoluble when expressed alone but became partially soluble when expressed with wild-type RPA32 and RPA14 (data not shown). In contrast, the DNA-binding domain polypeptides were soluble when expressed alone in *E. coli* (data not shown). [When sequences beyond residue 477 were expressed with the DNA-binding domain, e.g., RPA70(169–506), the polypeptides became insoluble (data not shown).] These data are consistent with previous studies which indicated that forms of RPA70 containing the C-terminal domain of RPA70 were insoluble in the absence of the two smaller subunits (43, 44).

All of the soluble mutant forms were purified to >95% homogeneity (Figure 2) and characterized using a combination of glycerol gradient sedimentation and gel permeation chromatography (data not shown). The hydrodynamic properties of the DNA-binding domain fragments indicated that these proteins were monomers in solution. The hydrodynamic parameters of aromatic residue mutants and RPA•70(Zn*) were equivalent to those of wild-type RPA, indicating that all are stable heterotrimeric complexes in solution. The one exception was RPA•70(F238A,W361A) which had a Stokes radius (55.8 ± 2.1 Å) slightly larger than wild-type RPA (51.8 ± 1.4 Å).

ssDNA-Binding Properties of Mutant Forms of RPA. Binding of the mutant forms of RPA to ssDNA was examined by gel mobility shift assays (GMSA). In these assays, a short oligonucleotide, (dT)₃₀, was incubated with a mutant form of RPA, and the protein–DNA complexes were separated by gel electrophoresis. This assay has the advantage of being able to detect binding over a wide range of affinities. Initial studies were carried out to determine the role of aromatic residues in RPA binding to ssDNA. Binding isotherms for two double mutants, RPA•70(F269A,F386A) and RPA•70(F238A,W361A), are shown in Figure 3A. RPA•70(F269A,F386A) and RPA•70(F238A,W361A) had affinities for ssDNA 1/10 and $\leq 1/500$ that of wild-type RPA, respectively (Figure 3A).² The apparent association constants determined in these experiments are summarized in Table 1. Because it was difficult to saturate binding with RPA•

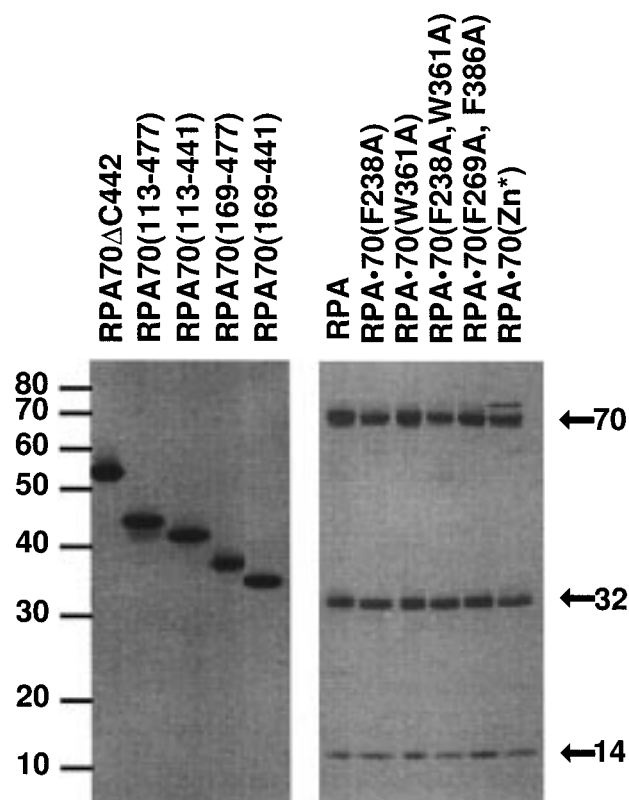


FIGURE 2: Purified RPA•70(Zn*), aromatic residue mutants, and DNA-binding domain polypeptides. A 0.5–1 μ g sample of RPA or the indicated mutant was electrophoresed on an 8–14% SDS–PAGE gel and visualized by staining with silver nitrate. Arrows indicate the positions of RPA70 (70), RPA32 (32), and RPA14 (14). The minor band at 71–72 kDa visible in some lanes is an *E. coli* protein contaminant. The positions of molecular mass standards in kDa are indicated.

70(F238A,W361A), its association constant must be considered an upper limit of the true binding constant. The DNA-binding activity of RPA complexes in which single aromatic residues were mutated was also examined. RPA•70(F269A) and RPA•70(F386A) had binding constants equivalent to wild-type RPA (data not shown), and RPA•70(F238A) and RPA•70(W361A) had binding constants one-third and one-tenth that of wild-type RPA, respectively (Figure 3B, see also Table 1). In the crystal structure of the central DNA-binding domain, all four of these aromatic residues stack with bases in the DNA. However, the modest changes observed with most of the aromatic residue mutants demonstrate that individually these residues are not essential for ssDNA-binding activity. Furthermore, the reduction in ssDNA-binding activity observed with the double-mutant RPA•70(F238A,W361A) was much greater than that for any single mutant alone or RPA•70(F269A,F386A). This indicates that residues F238 and W361 are not equivalent to F269 and F386 and that the presence of either F238 or W361 is sufficient for high-affinity ssDNA-binding activity of RPA. These studies also confirm that the central DNA-binding domain is necessary for ssDNA-binding activity.

² RPA•70(F269A,F386A) has three amino acid changes: F269A, F386A, and T270S. The conservative threonine to serine mutation was made to simplify creation of this mutant form of RPA. Biochemical analysis of RPA•70(F269A,F386A) and RPA•70(F269A,T270S) indicated that the T270S had no detectable effect on RPA function.

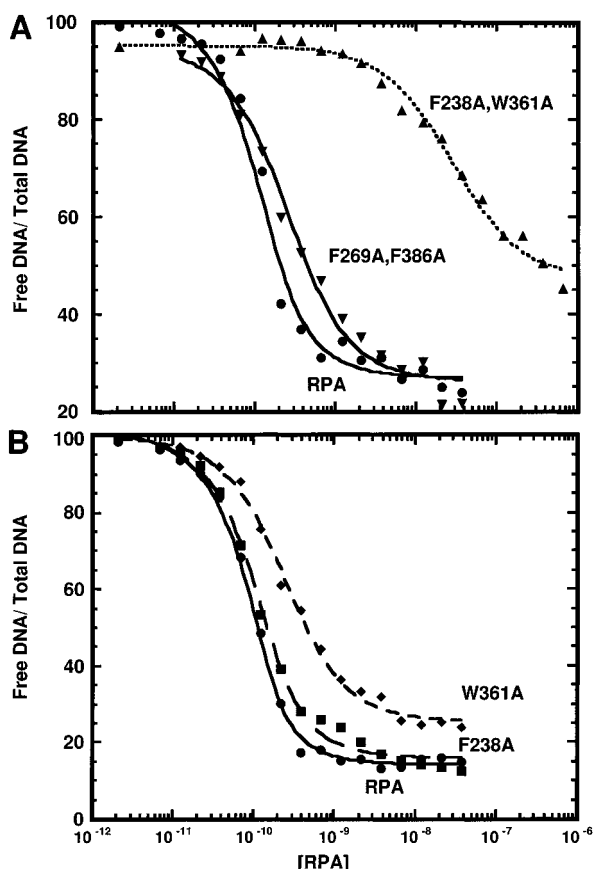


FIGURE 3: Binding isotherms for aromatic residue mutants. Binding to (dT)₃₀ was determined by GMSA. Binding data and best-fit curves for (A) RPA, RPA-70(F238A,W361A), and RPA-70(F269A,F386A); and (B) RPA, RPA-70(F238A), and RPA-70(W361A) are as indicated. The binding constants determined are summarized in Table 1. Multiple assays were performed, and representative data are shown. Titrations do not end at zero because of gel background.

Table 1: DNA-Binding Properties of RPA Mutants^a

form of RPA	$K_a[(dT)_{30}]$ ($\times 10^{-8} \text{ M}^{-1}$)	relative binding, $K_a/K_{a,\text{wildtype}}$
RPA	270 \pm 40 (S)	1
RPA70 Δ C442	21 \pm 8	0.08
RPA70 Δ C326	0.42 \pm 0.04	0.002
RPA-70(F238A,W361A)	0.66 \pm 0.09	0.002
RPA-70(F238A)	180 \pm 27	0.67
RPA-70(W361A)	43 \pm 7	0.16
RPA-70(F269A,F386A)	35 \pm 8	0.13
RPA70(113–477)	4.4 \pm 0.7	0.016
RPA70(113–441)	12 \pm 2	0.044
RPA70(169–477)	1.1 \pm 0.2	0.004
RPA70(169–441)	0.8 \pm 0.2	0.003
RPA-70(Zn ²⁺)	29 \pm 9	0.11

^a The average apparent association constant from multiple independent titrations is shown; errors were calculated using the standard formulation of determining propagation of individual errors obtained during nonlinear least-squares fitting. (S), stoichiometric or near-stoichiometric binding conditions.

To determine whether the central DNA-binding domain of RPA70 is sufficient for RPA-binding activity, DNA-binding domain polypeptides were assayed. Table 1 compares the apparent association constants determined for these mutant forms of RPA to those of selected deletions of RPA70. (All forms of RPA are shown schematically in Figure 1.) The DNA-binding domain polypeptides all had

reduced affinity for ssDNA; apparent association constants ranged between 1/20 and 1/300 that of wild-type RPA. The minimal DNA-binding domain mutant [RPA70(169–441)] had the lowest affinity for ssDNA. [The only previous analysis of the DNA-binding domain concluded that it had a higher affinity for ssDNA than shown here. However, those studies were carried out under stoichiometric binding conditions which precluded the accurate determination of equilibrium binding constants (49).] A drop in affinity was observed between RPA70(113–477) and RPA70(169–477) and between RPA70(113–441) and RPA70(169–441). This indicated that residues 113–168 were important for optimal binding of the DNA-binding domain. RPA70(113–441) had a higher affinity for ssDNA than did RPA70(113–477) while RPA70(168–441) and RPA70(168–477) had similar affinities. This suggests that in some contexts, residues 442–477 can have a modest inhibitory effect on ssDNA binding. We conclude that the central DNA-binding domain is necessary and sufficient for ssDNA-binding activity but that additional sequences are needed for optimal binding activity.

The putative zinc-finger domain also has a role in RPA–DNA interactions. The apparent association constant for RPA-70(Zn²⁺) was one-tenth that of wild-type RPA (Table 1). Previously, we have shown that deletion of the C-terminus of RPA70 up to the boundary of the ssDNA-binding domain (residue ~442) reduces the affinity of RPA by approximately an order of magnitude (44; see also Table 1). Thus, mutation of the putative zinc-finger motif had the same effect on ssDNA binding as deletion of RPA32/14 and residues 442–616 of RPA70. This suggests that the decrease in binding affinity observed with RPA70 Δ C442 can be attributed to the loss of the putative zinc finger and not to the loss of the 32- and 14-kDa subunits. We conclude that both the sequences immediately preceding the central DNA-binding domain (residues 113–168) and the putative zinc-finger domain are needed for maximal binding of RPA to ssDNA.

Structural Analysis of Mutant Forms of RPA. Whenever a mutation is made in a protein it is possible that the mutation affects the structure of the protein, its function, or both. Proteolytic enzymes directly interact with peptide bonds and provide a means to directly probe the structure of a protein. Therefore, we carried out partial proteolytic digestion of the mutant RPA complexes to determine whether these mutations caused significant changes in RPA structure. Previously, we have shown that treatment of RPA with proteases results in a limited and reproducible set of proteolytic fragments (45). When similar analysis was carried out using RPA-70-(F269A,F386A) and RPA-70(F238A,W361A), the initial digestion products observed were similar to those observed for wild-type RPA (Figure 4A). These data and the hydrodynamic analysis described above indicate that the global structure of both double mutants is similar to that of wild type. However, RPA-70(F238A,W361A) was digested more rapidly than either wild-type RPA or RPA-70(F269A,-F386A). This suggests that although mutation of F238 and W361 does not disrupt the global structure of the complex, it does cause a perturbation or destabilization of the RPA structure. These results are consistent with the observation that RPA-70(F238A,W361A) has a slightly larger Stokes radius than either wild-type RPA or RPA-70(F269A,F386A). When the single mutants RPA-70(F238A) and RPA-70-(W361A) were subjected to proteolysis, they were found to

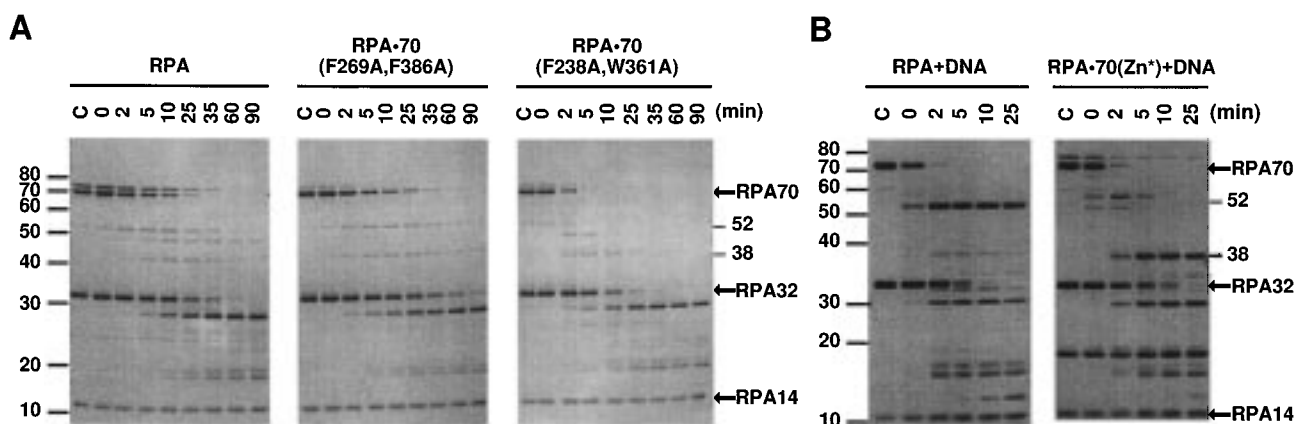


FIGURE 4: Partial proteolysis of specific RPA mutants. The indicated forms of RPA [wild-type RPA (RPA), RPA-70(F269A,F386A), RPA-70(F269A,F386A), RPA-70(Zn*)] were incubated with trypsin for the times indicated without DNA (A) or with 125 fmol of oligo-(dT)₃₀ (B; +DNA). Partial proteolysis was carried out as described previously (45). Briefly, 10 μ g of the indicated RPA complex was incubated with 50 ng of trypsin in 50 μ L of HI buffer at 37 $^{\circ}$ C. At the times indicated, aliquots containing \sim 1 μ g of protein were removed, and proteolysis was terminated by boiling for 5 min in sample loading buffer. Proteolyzed products were separated on an 8–14% SDS–polyacrylamide gel (SDS–PAGE) (62) and stained with silver nitrate (41). Lanes C contain undigested protein. The positions of the molecular mass markers are shown on the left (in kDa). The positions of the subunits (arrows) and the molecular mass in kDa of the major proteolytic fragments observed are indicated on the right. Representative digestions are shown. These results were confirmed in independent experiments.

give a similar digestion pattern with rates of digestion between those of wild-type and RPA-70(F238A,W361A). We conclude that aromatic residues F238 and W361 are important for maintaining the structure of the high-affinity DNA-binding domain. Mutation of either residue alone causes a small perturbation of the structure (and ssDNA-binding) while mutation of both residues causes a disruption of structure that has major effects on RPA activity.

The mutant RPA-70(Zn*) complex was also subjected to a partial proteolysis using trypsin. In the absence of ssDNA, the rate of digestion and the initial digestion products observed with RPA-70(Zn*) were similar to those of wild-type RPA (data not shown). We have shown previously that binding to ssDNA causes changes in the digestion pattern of wild-type RPA: RPA70 becomes more resistant and RPA32 becomes more sensitive to digestion. When RPA-70(Zn*) was incubated with ssDNA, similar changes were observed except that the major sites of cleavage changed. In the presence of ssDNA, wild-type RPA70 was rapidly cleaved to yield \sim 52-kDa and \sim 18-kDa fragments which were highly resistant to further digestion (Figure 4B). With RPA-70(Zn*), the \sim 52-kDa fragments were observed only transiently, and instead a \sim 38-kDa trypsin-resistant fragment was observed (Figure 4B). Also a ssDNA-dependent increase in the sensitivity of RPA32 was not observed with the RPA-70(Zn*) complex (Figure 4B). The cleavage sites of RPA-70(Zn*) were mapped by immunoblotting as described previously (45) (data not shown). This analysis indicated that the initial cleavage of the 70-kDa subunit of RPA-70(Zn*) occurred near the N-terminus-generated \sim 52-kDa and \sim 18-kDa fragments (as in wild type). The \sim 52-kDa fragment was then rapidly digested to a 38-kDa fragment which was resistant to further digestion. The position of this second cleavage site is near the putative zinc-finger motif. We conclude that mutation of the zinc-finger motif alters the structure of the 70-kDa subunit near the site of the mutation.

SV40 Replication Activity. We determined the activity of the mutant forms of RPA in SV40 replication. A series of replication assays were performed under conditions where DNA synthesis is absolutely dependent on both T antigen

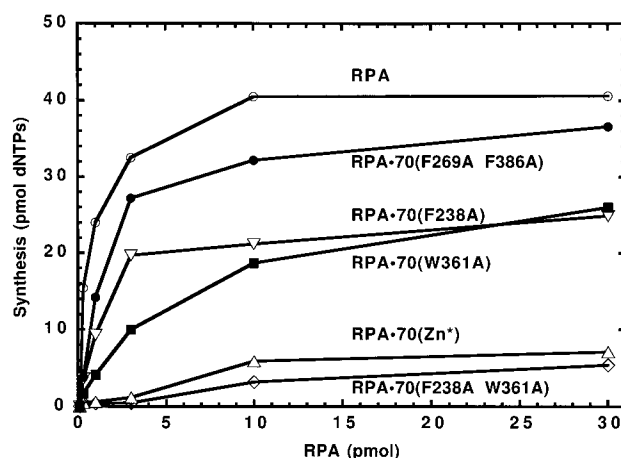


FIGURE 5: Replication activity of mutant forms of RPA. SV40 replication assays were carried out as described previously (42, 63). Cellular components necessary for SV40 replication were supplied as either purified or partially purified proteins. Each replication reaction contained 9.4 μ g of fraction CFII (containing DNA polymerases α and δ and RF-C), 4.2 μ g of fraction CFIBC (containing proliferating cell nuclear antigen and protein phosphatase 2A), 1 μ g of T antigen, and 1 unit of topoisomerase I. Wild-type or individual mutant forms of RPA were added as indicated. The assays were incubated for 2 h at 37 $^{\circ}$ C and the picomoles of dNTP incorporated was quantitated by TCA precipitation. Replication products were analyzed on agarose gels in independent experiments and found to be identical with all forms of RPA. DNA synthesis in the absence of added RPA was 0.8 pmol and in the absence of T antigen (with 3 pmol of RPA) was 1.0 pmol.

and functional RPA (Figure 5). None of the DNA-binding domain polypeptides were able to support SV40 replication (data not shown). All aromatic residue mutants except RPA-70(F238A,W361A) were able to support replication (Figure 5). RPA-70(F238A,W361A) has minimal ssDNA-binding activity, so its inability to support significant levels of DNA replication was not surprising. The other aromatic residue mutants, RPA-70(F269A,F386A), RPA-70(F238A), and RPA-70(W361A), all had binding constants within 1 order of magnitude of RPA yet had different activities in SV40 DNA replication (Figure 5). Specific activities range from ap-

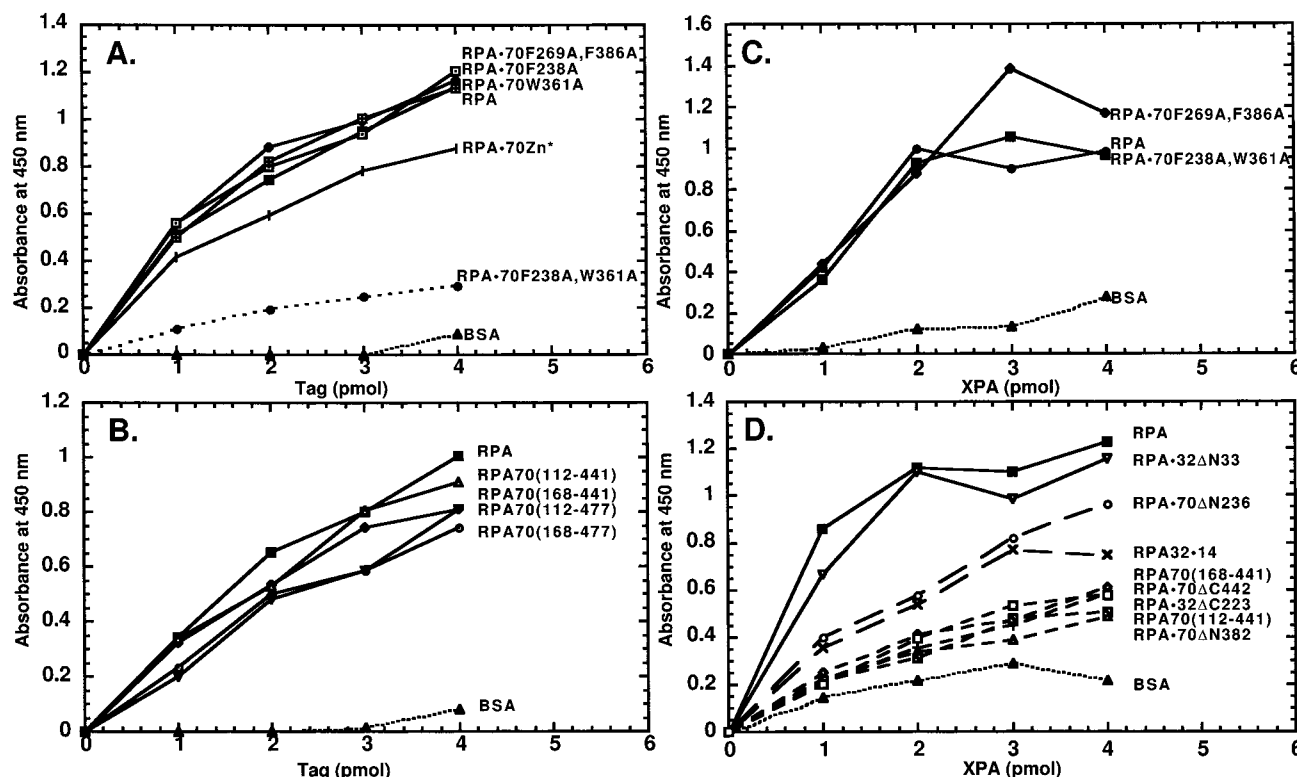


FIGURE 6: Protein interactions of mutant forms of RPA as monitored by ELISA. Wild-type or the indicated mutant form of RPA was immobilized on microtiter plates. Interactions with SV40 T antigen (A, B) or XPA (C, D) were then determined as described under Materials and Methods. Data shown are from a 20 min incubation with substrate. Multiple assays were performed, and representative data are shown. The absolute values varied between assays, but the relative signals for the different mutants were consistent. Lines corresponding to individual forms of RPA are indicated in the figure. Solid lines indicate interactions similar to wild-type RPA, dotted lines indicate background with bovine serum albumin (BSA), and dashed lines indicate intermediate interactions. SV40 large T antigen was purified as described previously (22). Histidine-tagged XPA was purified from *E. coli* as described previously (64). Either anti-T antigen or anti-polyhistidine antibodies were used as primary antibodies.

proximately 85% [RPA-70(F269A,F386A)] to ~50% [RPA-70(W361A)] that of wild-type RPA at saturation. For these mutant forms, replication activity did not directly correspond to ssDNA-binding activity. RPA-70(F238A) had the highest affinity for ssDNA and intermediate replication activity. Also, the replication activity of RPA-70(W361A) was ~50% that of RPA-70(F269A,F386A); these two forms have identical affinities for ssDNA. We conclude that while ssDNA-binding activity is essential for replication, other activities of RPA are also important for activity in replication. These conclusions are supported by the analysis of RPA-70(Zn*). RPA-70(Zn*) has an association constant that is equivalent to RPA-70(W361A) and RPA-70(F269A,F386A) (one-tenth that of wild-type RPA); however, it was defective in DNA replication even when high levels of protein were used (Figure 5). RPA-70(Zn*) also did not inhibit DNA synthesis when mixed with wild-type RPA (data not shown). We conclude that while only minimally involved in ssDNA binding, the zinc-finger motif is essential for activity in DNA replication.

RPA Interactions with XPA and SV40 T Antigen. RPA-protein interactions are believed to be important for RPA function. Therefore, the mutant forms of RPA were analyzed for their ability to interact with SV40 T antigen in ELISA assays. SV40 T antigen is essential for the initiation of SV40 DNA replication (50). We found that both the DNA-binding domain polypeptides and RPA-70(Zn*) were able to interact strongly with SV40 T antigen (Figure 6A,B). These results were consistent with previous studies which mapped T

antigen interactions to the N-terminal half of the central DNA-binding domain (1, 22) and indicated that mutation of the putative zinc-finger domain does not perturb the structure of this region of RPA. The aromatic residue mutants also interacted well with T antigen except for RPA-70(F238A,-W361A) which interacted very weakly (Figure 6A). These data support the conclusion that in this double mutation, the structure of the DNA-binding/T antigen interaction domain is partially disrupted. (Note that mutants with a single aromatic residue change interacted with T antigen normally, indicating that their structure is close to wild-type RPA.)

Interactions of these mutants with XPA were also examined. RPA-XPA interactions are thought to be important in the damage recognition step of nucleotide excision repair (1, 51–53). The mutant forms of RPA fell into three groups based on their interactions with XPA: forms of RPA that interacted at near-wild-type levels; those that interact with intermediate affinity; and those that interacted weakly (near background). The first group included the aromatic residue mutants, RPA-70(Zn*), and RPA-32ΔN33 which had the N-terminal 33 residues of RPA32 deleted (Figure 6C,D, and data not shown). The second group included a complex of 32- and 14-kDa subunits and N-terminal deletions of RPA70 in which amino acids up to residue 236 were deleted. Selected members of this group are shown in Figure 6D. The low-interacting group included C-terminal deletions of RPA70, C-terminal deletions of RPA32, and all the DNA-binding domain polypeptides (Figure 6D). These data are summarized in Figure 1. These data suggest that two regions

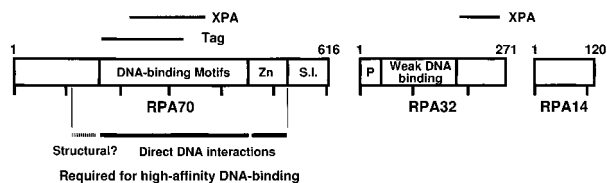


FIGURE 7: Schematic showing protein interaction domains and regions required for ssDNA binding. Functional domains are indicated in the schematic: Zn, zinc-finger domain; S.I., subunit interactions; P, phosphorylation/regulatory domain (1, 23). Horizontal lines above the schematic indicate sites of protein interaction: XPA and T antigen (Tag). Bars under the schematic indicate regions required for high-affinity ssDNA binding: dashed bar, probably contributes to the structure of the DNA-binding domain (Structural?); solid bars, directly interacting with DNA. See text for detailed discussion.

of RPA are involved in RPA–XPA interactions. The C-terminus of RPA32 seems to be the primary interaction site for XPA because deletion of 49–16 residues from the N-terminus of RPA32 caused a dramatic reduction in XPA interactions (Figure 6D, and data not shown). This domain is not the only interaction site because RPA32•14 and deletions missing only regions of RPA70 (RPA•70ΔN382) had reduced interactions with XPA. The finding that RPA•70ΔN236 interacted at an intermediate level but RPA•70ΔN382 interacted very poorly with XPA indicated that the second interaction site includes residues ~236–382. This second region does not seem to be sufficient for strong interactions with XPA because the DNA-binding domain polypeptides do not interact well with XPA. The regions of RPA that interact with T antigen and XPA are shown schematically in Figure 7.

DISCUSSION

We have shown that the central DNA-binding domain of RPA70 is necessary and sufficient for ssDNA-binding activity. However, this domain alone has an affinity for ssDNA that is more than 2 orders of magnitude lower than that of the heterotrimeric RPA complex [Table 1; see also (33, 49)]. Maximal binding activity requires sequences outside of the central DNA-binding domain (Figure 7). There are two possible mechanisms by which adjacent sequences could contribute to the affinity of RPA: direct interactions with DNA or contributing to the stability of the structure of the central DNA-binding domain. Our data support both processes occurring. Residues 113–168 cause the binding constant of the isolated central DNA-binding domain to increase by approximately 1 order of magnitude (Table 1); however, in the context of heterotrimeric RPA complex, these residues do not affect the affinity of RPA (44). This suggests that these residues have a structural role rather than directly interacting with the DNA. In contrast, the putative zinc-finger domain increases binding affinity by directly interacting with the DNA (see below).

All known homologues of RPA70 possess an identical C₄-type putative zinc-finger motif near residue 500 (1). Previous studies to define the role of this domain have been ambiguous. In one set of studies, mutation of two of the conserved cysteines inactivated RPA in SV40 DNA replication and base excision repair but did not affect nucleotide excision repair (36, 37). In contrast, a second laboratory found that a mutant, in which the zinc-finger domain was deleted, was active in

DNA replication but not active in nucleotide excision repair (38, 39). None of these studies quantitated the role of the putative zinc-finger domain on ssDNA-binding activity. Our data agree with the first set of studies (36, 37) and provide a mechanistic basis for this defect in function. We found that RPA containing mutations in the conserved cysteine residues had an affinity for ssDNA that was an order of magnitude lower than wild-type RPA and had a disruption of the structure of the C-terminal domain of RPA70. These changes were sufficient to cause a loss of activity in SV40 DNA replication but did not affect interactions with T antigen and XPA. Our conclusions are supported and extended in the accompanying paper which shows that the zinc-finger motif directly interacts with DNA and that metal ions are needed for function of the zinc-finger motif (54). In addition, recent studies by Brill and Bastin-Shanower have shown that the zinc-finger motif in the yeast homologue of RPA interacts with ssDNA (55). The structural perturbation observed in RPA•70(Zn*) may explain the inconsistencies between the previous studies of this domain. It is possible that deletion of the domain is less disruptive than making point mutations.

The zinc-finger motif in RPA70 is essential for function. However, the decrease in replication activity of RPA•70(Zn*) is greater than predicted by the change in ssDNA-binding activity (see Figure 5). In the accompanying paper, we show that the zinc-finger domain directly interacts with DNA (54). Thus, it is possible that these interactions are essential for RPA function in DNA replication. Alternatively, the perturbation of the structure caused by mutating the zinc-finger motif could disrupt the structure of some other region of RPA essential for function. The first hypothesis is supported by hydrodynamic analysis and partial proteolysis which showed that there were not large changes in the global structure of RPA•70(Zn*). Interestingly, the decreases in ssDNA-binding affinity and replication activity observed with RPA70ΔC442 which lacks the C-terminal 175 residues of the 70-kDa subunit (including the zinc-finger motif) and the entire 32- and 14-kDa subunits. This suggests that the major defect in RPA70ΔC442 is caused by the loss of the zinc-finger motif. It has been recently shown that a complex of RPA32/14 binds weakly to ssDNA (27, 31). However, the binding activity of RPA•70(Zn*) is most consistent with the 32- and 14-kDa subunits not contributing significantly to ssDNA-binding affinity of the heterotrimeric complex. Although, it is also possible that mutation of the zinc-finger motif somehow prevents the normal function of the 32- and 14-kDa subunits.

The crystal structure of the high-affinity binding domain bound to DNA suggested that both hydrophobic (base-stacking) interactions and ionic interactions were contributing to the stability of the RPA–DNA complex (33). Four aromatic residues (F238, F269, W361, and F386) interact with bases in the DNA. Mutant forms of RPA with mutations in individual hydrophobic residues or the double mutant RPA•70(F269A,F386A) all had minimal changes in ssDNA-binding activity; the binding constants for these mutants ranged from one-tenth to equal to that of wild-type RPA. In contrast, the double mutant RPA•70(F238A,W361A) had a binding constant that was 3 orders of magnitude lower than wild-type RPA; however, its structure was partially disrupted. Examination of the crystal structure of the central binding

domain indicated that residues F238 and W361 are closely packed with other residues (i.e., partially "buried") (33). In contrast, the side chains of F269 and F386 both extend away from other residues (33). These differences are consistent with mutation of F238 and W361 causing a greater disruption of the structure of the DNA-binding domain than mutation of F269 and F386. The structural perturbation seen in RPA-70(F238A,W361A) makes it difficult to draw firm conclusions about its mutant phenotype; however, it seems likely that the change in structure contributes to its lower ssDNA-binding activity. The other aromatic residue mutants suggest that no one aromatic residue is essential for formation of the RPA-DNA complex. Furthermore, these studies suggest that ionic interactions, not base stacking, are responsible for most of the energy of interaction between RPA and ssDNA. This conclusion is consistent with the strong ionic dependence of RPA binding to ssDNA (26, 56, 57) and also with studies of other single-stranded-binding proteins that show multiple ionic interactions (58, 59).

Philipova and co-workers identified four aromatic residues in the yeast homologue of RPA70 which were conserved between RPA homologues and *E. coli* single-stranded-binding protein (34). Of these four residues, only two correspond to residues that directly interact with DNA in the crystal structure (equivalent to F238 and W361) (33). Mutation of these residues resulted in cells that were not viable. A simple explanation of this phenotype is that the mutation caused a disruption in RPA structure and decreased DNA-binding activity as observed in vitro (see above). While this seems likely to be the case, it should be noticed that the viability of single point mutations does not correlate directly with the biochemical analysis of these studies. We found that both single mutations had modest effects on DNA binding and DNA replication. However, yeast cells are viable when the residue corresponding to W361 was mutated but not viable when the residue corresponding to F238 was mutated. This discrepancy could be the result of the mutations effecting processes in vivo that have not been examined in vitro such as DNA repair or interactions with other proteins such as DNA polymerase α /primase. The latter possibility is supported by F238 being located in a protein interaction domain of RPA (22), making it likely that a mutation of this residue would affect essential RPA-protein interactions.

Mutant forms of RPA that had a significantly decreased ssDNA-binding activity were unable to support DNA replication. However, mutants with modest defects in ssDNA had different activities in DNA replication. These results are consistent with ssDNA-binding activity being necessary but not sufficient for RPA function in replication and with other activities of RPA being necessary [see also (1)].

These studies also confirm that the central DNA-binding domain of RPA70 participates directly in protein-protein interactions. Analysis of the interactions with XPA indicated that there are two XPA interaction domains on RPA. The first is near the C-terminus of RPA32, and the second is in the central domain of RPA70 (Figure 7). [The first domain as has been mapped previously (39, 52, 60).] XPA interaction domains on RPA are thus overlapping with, but not identical to, those for DNA polymerase α (22). Previously it has been shown that the N-terminal half of RPA70 interacts with multiple proteins (22). It now appears that the C-terminal

domain of RPA32 is a second general protein interaction domain which interacts with XPA, uracil-DNA glycosylase (61), and possibly other proteins.

ACKNOWLEDGMENT

We thank Xioyi Yao and Ting Liu for preliminary studies on the aromatic residue single mutants. We thank Aled Edwards for communication of results prior to their publication. We thank Richard Wood for the XPA expression plasmid. We thank the members of the Wold laboratory for scientific discussions and critical reading of the manuscript. We thank the University of Iowa DNA Core Facility for oligonucleotide synthesis and DNA sequencing.

REFERENCES

1. Wold, M. S. (1997) *Annu. Rev. Biochem.* 66, 61–92.
2. Fairman, M. P., and Stillman, B. (1988) *EMBO J.* 7, 1211–1218.
3. Wold, M. S., and Kelly, T. (1988) *Proc. Natl. Acad. Sci. U.S.A.* 85, 2523–2527.
4. Van der Knaap, E., Jagoueix, S., and Kende, H. (1997) *Proc. Natl. Acad. Sci. U.S.A.* 94, 9979–9983.
5. Brill, S. J., and Stillman, B. (1989) *Nature* 342, 92–95.
6. Brown, G. W., Melendy, T. E., and Ray, D. S. (1992) *Proc. Natl. Acad. Sci. U.S.A.* 89, 10227–10231.
7. Melendy, T., and Stillman, B. (1993) *J. Biol. Chem.* 268, 3389–3395.
8. Kamakaka, R. T., Kaufman, P. D., Stillman, B., Mitsis, P. G., and Kadonaga, J. T. (1994) *Mol. Cell. Biol.* 14, 5114–5122.
9. Dornreiter, I., Erdile, L. F., Gilbert, I. U., von Winkler, D., Kelly, T. J., and Fanning, E. (1992) *EMBO J.* 11, 769–776.
10. Coverley, D., Kenny, M. K., Lane, D. P., and Wood, R. D. (1992) *Nucleic Acids Res.* 20, 3873–3880.
11. Heyer, W.-D., Rao, M. R. S., Erdile, L. F., Kelly, T. J., and Kolodner, R. D. (1990) *EMBO J.* 9, 2321–2329.
12. Moore, S. P., Erdile, L., Kelly, T., and Fishel, R. (1991) *Proc. Natl. Acad. Sci. U.S.A.* 88, 9067–9071.
13. Sung, P. (1997) *J. Biol. Chem.* 272, 28194–28197.
14. Shinohara, A., and Ogawa, T. (1998) *Nature* 391, 404–407.
15. New, J. H., Sugiyama, T., Zaitseva, E., and Kowalczykowski, S. C. (1998) *Nature* 391, 407–410.
16. Sugiyama, T., New, J. H., and Kowalczykowski, S. C. (1998) *Proc. Natl. Acad. Sci. U.S.A.* 95, 6049–6054.
17. He, Z., Brinton, B. T., Greenblatt, J., Hassell, J. A., and Ingles, C. J. (1993) *Cell* 73, 1223–1232.
18. Li, R., and Botchan, M. R. (1993) *Cell* 73, 1207–1221.
19. Dutta, A., Ruppert, J. M., Aster, J. C., and Winchester, E. (1993) *Nature* 365, 79–82.
20. Abramova, N. A., Russell, J., Botchan, M., and Li, R. (1997) *Proc. Natl. Acad. Sci. U.S.A.* 94, 7186–7191.
21. Miller, S. D., Moses, K., Jayaraman, L., and Prives, C. (1997) *Mol. Cell. Biol.* 17, 2194–2201.
22. Braun, K. A., Lao, Y., He, Z., Ingles, C. J., and Wold, M. S. (1997) *Biochemistry* 36, 8443–8454.
23. Deleted in proof.
24. Kim, C., Snyder, R. O., and Wold, M. S. (1992) *Mol. Cell. Biol.* 12, 3050–3059.
25. Kim, C., Paulus, B. F., and Wold, M. S. (1994) *Biochemistry* 33, 14197–14206.
26. Kim, C., and Wold, M. S. (1995) *Biochemistry* 34, 2058–2064.
27. Sibenaller, Z. A., Sorensen, B. R., and Wold, M. S. (1998) *Biochemistry* 37, 12496–12506.
28. Blackwell, L. J., and Borowiec, J. A. (1994) *Mol. Cell. Biol.* 14, 3993–4001.
29. Blackwell, L. J., Borowiec, J. A., and Mastrangelo, I. A. (1996) *Mol. Cell. Biol.* 16, 4798–4807.
30. Lavrik, O. I., Nasheuer, H. P., Weisschart, K., Wold, M. S., Prasad, R., Beard, W. A., Wilson, S. H., and Favre, A. (1998) *Nucleic Acids Res.* 26, 602–607.

31. Bochkareva, E., Frappier, L., Edwards, A. M., and Bochkarev, A. (1998) *J. Biol. Chem.* 273, 3932–3936.
32. Mass, G., Nethanel, T., and Kaufmann, G. (1998) *Mol. Cell. Biol.* 18, 6399–6407.
33. Bochkarev, A., Pfuetzner, R. A., Edwards, A. M., and Frappier, L. (1997) *Nature* 385, 176–181.
34. Philipova, D., Mullen, J. R., Maniar, H. S., Gu, C., and Brill, S. J. (1996) *Genes Dev.* 10, 2222–2233.
35. Burns, J. L., Guzder, S. N., Sung, P., Prakash, S., and Prakash, L. (1996) *J. Biol. Chem.* 271, 11607–11610.
36. Lin, Y. L., Chen, C., Keshav, K. F., Winchester, E., and Dutta, A. (1996) *J. Biol. Chem.* 271, 17190–17198.
37. Lin, Y. L., Shivji, M. K. K., Chen, C., Kolodner, R., Wood, R. D., and Dutta, A. (1998) *J. Biol. Chem.* 273, 1453–1461.
38. Kim, D. K., Stigger, E., and Lee, S. H. (1996) *J. Biol. Chem.* 271, 15124–15129.
39. Stigger, E., Drissi, R., and Lee, S. H. (1998) *J. Biol. Chem.* 273, 9337–9343.
40. Studier, F. W., Rosenberg, A. H., Dunn, J. J., and Dubendorff, J. W. (1990) *Methods Enzymol.* 185, 60–89.
41. Ausubel, F. M., Brent, R., Kingston, R. E., Moore, D. D., Seidman, J. G., Smith, J. A., and Struhl, K. (1989) in *Current protocols in molecular biology*, John Wiley and Sons, New York.
42. Henricksen, L. A., Umbricht, C. B., and Wold, M. S. (1994) *J. Biol. Chem.* 269, 11121–11132.
43. Gomes, X. V., and Wold, M. S. (1995) *J. Biol. Chem.* 270, 4534–4543.
44. Gomes, X. V., and Wold, M. S. (1996) *Biochemistry* 35, 10558–10568.
45. Gomes, X. V., Henricksen, L. A., and Wold, M. S. (1996) *Biochemistry* 35, 5586–5595.
46. Bradford, M. M. (1976) *Anal. Biochem.* 72, 248–254.
47. Dornreiter, I., Höss, A., Arthur, A. K., and Fanning, E. (1990) *EMBO J.* 9, 3329–3336.
48. Harlow, E., Crawford, L. V., Pim, D. C., and Williamson, N. M. (1981) *J. Virol.* 39, 861–869.
49. Pfuetzner, R. A., Bochkarev, A., Frappier, L., and Edwards, A. M. (1997) *J. Biol. Chem.* 272, 430–434.
50. Hassell, J. A., and Brinton, B. T. (1996) in *DNA Replication in Eukaryotic Cells* (DePamphilis, M. L., Ed.) pp 639–677, Cold Spring Harbor Laboratory Press, Cold Spring Harbor, NY.
51. Clugston, C. K., McLaughlin, K., Kenny, M. K., and Brown, R. (1992) *Cancer Res.* 52, 6375–6379.
52. Li, L., Lu, X. Y., Peterson, C. A., and Legerski, R. J. (1995) *Mol. Cell. Biol.* 15, 5396–5402.
53. He, Z., Henricksen, L. A., Wold, M. S., and Ingles, C. J. (1995) *Nature* 374, 566–569.
54. Lao, Y., Lee, C. G., and Wold, M. S. (1999) *Biochemistry* 38, 3974–3984.
55. Brill, S. J., and Bastin-Shanower, S. (1998) *Mol. Cell. Biol.* 18, 7225–7234.
56. Alani, E., Thresher, R., Griffith, J. D., and Kolodner, R. D. (1992) *J. Mol. Biol.* 227, 54–71.
57. Mitsis, P. G., Kowalczykowski, S. C., and Lehman, I. R. (1993) *Biochemistry* 32, 5257–5266.
58. Revzin, A. (1990) in *The Biology of Nonspecific DNA–Protein Interactions*, CRC Press, Boca Raton.
59. Lohman, T. M., and Ferrari, M. E. (1994) *Annu. Rev. Biochem.* 63, 527–570.
60. Matsuda, T., Saijo, M., Kuraoka, I., Kobayashi, T., Nakatsu, Y., Nagai, A., Enjoji, T., Masutani, C., Sugawara, K., Hanaoka, F., Yasui, A., and Tanaka, K. (1995) *J. Biol. Chem.* 270, 4152–4157.
61. Nagelhus, T. A., Haug, T., Singh, K. K., Keshav, K. F., Skorpen, F., Otterlei, M., Bharati, S., Lindmo, T., Benichou, S., Benarous, R., and Krokan, H. E. (1997) *J. Biol. Chem.* 272, 6561–6566.
62. Laemmli, U. K. (1970) *Nature* 227, 680–685.
63. Wold, M. S., Weinberg, D. H., Virshup, D. M., Li, J. J., and Kelly, T. J. (1989) *J. Biol. Chem.* 264, 2801–2809.
64. Jones, C. J., and Wood, R. D. (1993) *Biochemistry* 32, 12096–12104.

BI982370U